Cupric Oxide-Coated PCB-based Interdigitated Transducer for Acetone Sensing

2025 Symposium on Design, Test, Integration and Packaging of MEMS/MOEMS (DTIP) | 978-1-6654-7794-9/25/$31.00 ©2025 IEEE | DOI: 10.1109/DTIP66728.2025.11099216

Nermine Zardi
SMALL Research Group, ICTEAM Institute, UCLouvain, Belgium
SI2E Laboratory, École nationale d'ingénieurs de Sfax, Université de Sfax, Tunisia
nermine.zardi@uclouvain.be

Shirin Afyouni
R&D department
VOCSens srl
Belgium
Shirin.afyouni@vocsens.com

Mohamed Masmoudi
SI2E Laboratory, École nationale d'ingénieurs de Sfax, Université de Sfax, Tunisia
mohamed.masmoudi@enis.tn

Yann Danlée
Management dpt.
VOCSens srl
Belgium
yann.danlee@vocsens.com

Farès Tounsi
SMALL Research Group, ICTEAM Institute, UCLouvain, Belgium
SI2E Laboratory, École nationale d'ingénieurs de Sfax, Université de Sfax, Tunisia
fares.tounsi@uclouvain.be

Denis Flandre
SMALL Research Group, ICTEAM Institute, UCLouvain,
Belgium
denis.flandre@uclouvain.be

***Abstract*—In this paper, we report a copper oxide (CuO)-coated gas sensor based on an interdigitated capacitive transducer for the detection of volatile organic compounds (VOCs), especially acetone. The device is built on a printed circuit board (PCB) as a gold-copper interdigitated capacitor (20 fingers, 0.4 mm electrode width, 0.2 mm gap), functionalized with a sputtered CuO sensitive layer, which was selected for its stability, non-toxicity, cost-effectiveness, and durability. Finite element simulations using COMSOL were used to model the capacitance of the fabricated sensor and were validated by analytical estimation. CuO was deposited via DC magnetron sputtering at room temperature. Its structural characterization was carried out by Raman spectroscopy, and SEM demonstrated the successful deposition. Electrical measurements using a vector network analyzer (VNA) assessed the changes in capacitance and resistance versus frequency, both with the sensitive layer and under acetone exposure. The effects of CuO and acetone were observed in terms of the changes in capacitance and resistance.**

Keywords—gas sensing, interdigitated capacitor, cupric oxide, electric measurements, acetone.

I. Introduction

Gas sensors are widely used in industrial safety, environmental monitoring, medical diagnostics, and smart home devices. Although acetone is widely used in chemistry and industry, it is a toxic volatile organic compound that can pose health and environmental risks, especially under prolonged exposure [1]. Therefore, its detection and monitoring are of paramount importance. Gas detectors based on printed circuit boards (PCBs) are widely used due to their advantages. PCBs, especially FR-4, made of fiberglass and epoxy resin, are cost effective and relatively inexpensive compared to more specialized substrates (e.g., silicon, low-temperature Co-fired ceramic (LTCC), among others.) [2, 3]. These boards (typically 1.6 mm thick) offer decent mechanical strength, ensuring that the sensor structure remains intact during regular use and handling. They also provide good electrical insulation properties, which are essential in any sensor circuit. This helps prevent electrical interference and ensures the stability of the signal processing components used in detecting gas concentrations [3, 4]. On the other hand, a gas sensor consists of two basic components: the transducer and the active layer. The active layer is the component that interacts directly with the target gas molecules. The transducer is the component that converts the physical interaction between the target gas and the sensitive layer into changes in electrical parameters such as resistance, capacitance, or inductance.

Bamiedakis *et al.* [4] constructed an ammonia (NH_3)-sensitive bromocresol purple (BCP) and bromothymol blue (BTB) sensor based on PCB substrate. They investigated the evolution of the optical transmission characteristics of chemically functionalized optical waveguides in the presence of NH_3 molecules. The device achieved a sensitivity of about 30 ppm and a response of up to 600 ppm at room temperature. Said *et al.* [5] published a paper for carbon dioxide (CO_2) sensing based on graphene oxide (GO)-coated spiral inductor on PCB substrate. The sensor showed a reduction in series inductance and resistance by approximately 9.33 % and 31 %, respectively. Interdigitated capacitors (IDC) are commonly utilized transducers in gas detection due to their low-cost, ease of fabrication, and high sensitivity [6-13]. Prezioso *et al.* [8] demonstrated an interdigitated-GO sensor for nitrogen dioxide detection. GO was deposited on 30 µm spaced interdigitated Platine (Pt) electrodes patterned on silicon nitride (Si_3N_4) substrate. The device was stable, had a lifetime of more than 1000 s hours, and exhibits a very low detection limit (20 ppb). Akhter *et al.* [12], fabricated a CO_2 sensor based on an interdigitated structure and a graphene oxide as the sensitive layer, for a concentration range of 400 ppm to 4000 ppm. The sensor dimensions and sensitive area were 10 mm × 10 mm and 6.25 mm^2, respectively. The sensor was highly responsive, with a response time and recovery time of 3 s and 5 s, respectively.

Cupric oxide (CuO) is a promising material for the sensitive layer due to its properties such as high stability, accessibility, and antibacterial activity [14]. Furthermore, it was chosen based on the fact that gas adsorption on semiconductors causes a change in their electrical conductivity, as well as a change in

978-1-6654-7794-9/25/$31.00 ©2025 IEEE

permittivity, when exposed to the target gas atmospheres, which may lead to a change in the capacitance of the interdigitated structure. Szkudlarek *et al.* [15], developed a Cr-doped CuO interdigitated resistive sensor for acetone detection in the range of 0.4 ppm to 3.2 ppm at 50 % of relative humidity (RH) measured at different temperatures. The response time and recovery time at 3.2 ppm were 35 s and 65 s, respectively. Mullen and Dutta [11], developed a resistive sensor for nitrogen dioxide (NO_2) and nitric oxide (NO) made of cupric oxide (CuO), which was deposited on the surface of an alumina substrate with interdigitated gold electrodes. Each electrode contained 10 interdigits. The gap between interdigits and their thickness were both 250 microns. CuO exhibited higher selectivity for NO than for NO_2 at 300°C. To our knowledge, capacitance variations are rarely exploited in literature, where the resistance response is mostly studied for gas sensing.

In this work, we fabricated a CuO-based IDC sensor for acetone gas detecting. The electrical response of this sensor was successfully analyzed in the frequency range of 100 kHz to 3 GHz for the blank, CuO-covered, and acetone-exposed structures. The sensitivity of copper oxide to acetone at a concentration of 1 L/min was studied.

II. Methods and Materials

A. The IDC fabrication and computing

The IDC consists of 35 µm-thick gold-coated copper electrodes, fabricated on a 1.6 mm-thick FR-4 PCB substrate. Fig. 1 shows the top view of the IDC with the geometric dimensions explained, while TABLE I lists them. In this structure, the black comb-shaped electrodes are interconnected, while the gray electrodes are also interconnected. The lumped-element electric circuit of the structure is given by a capacitance (C_{eff}) connected in parallel with a resistance (R_d), which accounts for dielectric losses. These elements are connected in series with a resistance (R_s), which represents the parasitic losses, and an inductance (L_s) associated with the long leads of the input and output electrodes [16]. This arrangement is illustrated in Fig. 2. The real part of the total equivalent impedance of the circuit *Re(Z)*, the imaginary part *Im(Z),* and the quality factor *(Q)* expressions are given, respectively, in (1), (2), and (3), as:

$$\mathrm{Re(Z)}=\frac{R_s+R_d+R_sR_d^2C_{eff}^2\omega^2}{1+R_d^2C_{eff}^2\omega^2} \quad (1)$$

$$\mathrm{Im(Z)}=\frac{\omega\,(L_s-R_d^2C_{eff}+R_d^2L_sC_{eff}^2\omega^2)}{1+R_d^2C_{eff}^2\omega^2} \quad (2)$$

$$\mathrm{Q}=\frac{\mathrm{Im(Z)}}{\mathrm{Re(Z)}}=\frac{\omega\,(L_s-R_d^2C_{eff}+R_d^2L_sC_{eff}^2\omega^2)}{R_s+R_d+R_sR_d^2C_{eff}^2\omega^2} \quad (3)$$

The analytical value of the capacitance was calculated using the theoretical conformal mapping method [17]. Its configuration is represented in Fig. 3, and the appropriate total capacitance calculation is described as:

$$C_{IDC}=(N-3)\frac{C_I}{2}+2\,\frac{C_I\times C_E}{C_I+C_E} \quad (4)$$

where C_I and C_E are the capacitances between the internal and external electrodes, respectively, with the total number of electrodes, N, being greater than three. The internal capacitance (C_I) and external capacitance (C_E) of the IDC are calculated based on the elliptic function K as detailed below:

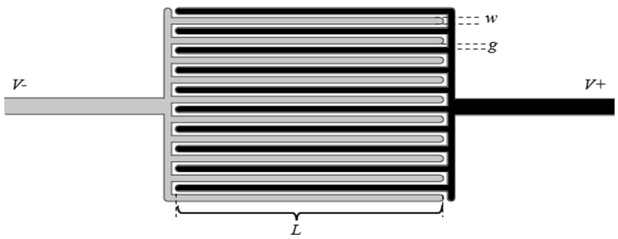

Fig. 1. Interdigitated capacitor's geometry.

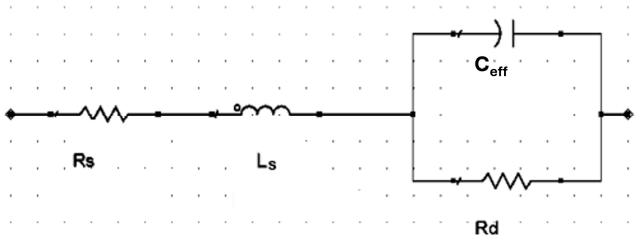

Fig. 2. Equivalent electric model of interdigitated capacitance.

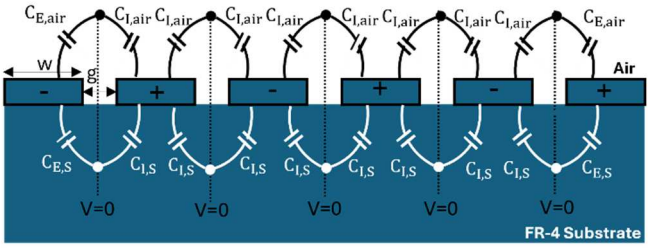

Fig. 3. Cross-section of a six-electrode interdigitated structure including the interior and exterior capacitances for both air and FR-4 substrate layers.

TABLE I. Dimensions of the IDC Geometry.

Geometrical parameters	Electrode width *w* (mm)	Electrode length *L* (mm)	Gap between electrodes *g* (mm)	Electrodes' number N
Values	0.4	14.2	0.2	20

$$C_I=C_{I,\,air}+C_{I,S}=\varepsilon_0 L\left(\frac{K(k_{I,\infty})}{K(k'_{I,\infty})}+\varepsilon_S\frac{K(k_{I,S})}{K(k'_{I,S})}\right) \quad (5)$$

$$C_E=C_{E,\,air}+C_{E,S}=\varepsilon_0 L\left(\frac{K(k_{E,\infty})}{K(k'_{E,\infty})}+\varepsilon_S\frac{K(k_{E,S})}{K(k'_{E,S})}\right) \quad (6)$$

where $C_{I,air}$ and $C_{I,S}$ are the interior capacitances through air and FR-4 substrate, respectively, $C_{E,air}$ and $C_{E,S}$ are the exterior capacitances through air and FR-4 substrate, while the quantities $k_{I,\infty}$, $k_{I,S}$, $k_{E,\infty}$, and $k_{E,S}$ are given in Appendix B: Table 2 of [17]. The permittivities of air and FR-4 (ε_S) were set to 1 and 4.6, respectively, giving a theoretical capacitance value C_{IDC} of 9.79 pF.

B. IDC numerical simulation

The physical model of the IDC-based sensor with its specific geometrical parameters was simulated using the finite element software COMSOL Multiphysics [18]. The electrostatic study was selected in the AC/DC module, and then the material properties, air block volume, interdigitated electrodes, and PCB substrate mass were defined. A DC voltage of 1V was applied to one set of excitation electrodes,

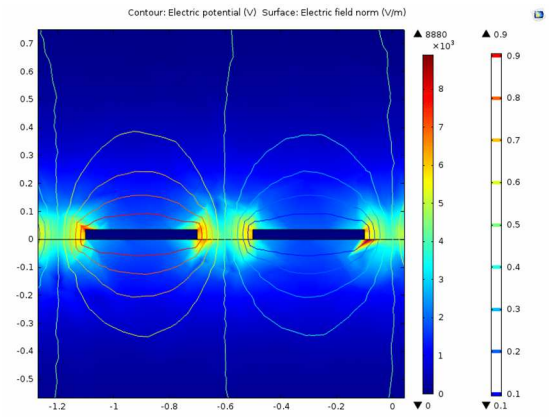

Fig. 4. Electric field and electric potential distributions in the IDC.

while the other set was grounded [6]. Next, a suitable mesh was selected for the main structure, and finally, a simulation was performed to analyze the IDC capacitance. The analytical capacitance value was validated against the simulated value of 10.16 pF (Fig. 4), resulting in a relative error of 3.7%. This can be attributed to material losses, such as resistive losses. Fig. 4 illustrates the distribution of the electric field and electric potential within the IDC structure. The electric field is concentrated between and around the interdigitated fingers, and its highest intensity is observed in the gaps between adjacent electrodes of opposite potentials. The colour legend on the right corresponds to the electric potential, while the one on the left represents the electric field.

C. Sensitive layer deposition and characterization

The CuO layer was deposited by DC magnetron sputtering technique, using AJA equipment available at the WINFAB micro-nano fabrication platform at UCLouvain, on a bare silicon wafer at room temperature under a pressure of 5 mTorr, a concentration of 30 sccm of oxygen (O_2) and argon (Ar), and a power of 50 W [19]. The deposition took about 1 hour to reach a thickness of 300 nm for CuO. The substrate was characterized by a Raman spectroscope with green radiation (acquisition time: 100 s, accumulation: 2, and power: 25 %) and a scanning electron microscope.

Fig. 5a presents the Raman spectra of CuO with three main peaks at 296.142 nm, 343.895 nm, and 626.743 nm [20]. The Si peak (519.642 nm) appears due to the strength of silicon even at a shorter wavelength (The Si peak also appears with red radiation). Fig. 5b shows the nanostructure of the CuO using a Zeiss Auriga dual beam FIB-SEM system. The structure of the CuO is characterized by cylindrical and elongated grains. These results confirm the successful deposition of high-quality cupric oxide. Subsequently, to collect the electrical properties (especially the resistivity), the four-points probe shown in Fig. 6, available at the WELCOME platform within the ICTEAM group, was used. It showed that the resistivity value of the cupric oxide sheet was 304 Ω·m.

III. Results and Discussion

The IDC-based sensor manufactured on FR-4 is shown in Fig. 7. Cupric oxide (in black) was deposited on the surface of the interdigitated gold-plated copper structure (in yellow). The extra surface (the surrounding ground plane and SMA footprints) was covered with Kapton and subsequently removed. The deposited CuO layer was 1 µm (approximately 3 hours of deposition), overlaying the 35 µm-thick metal layer.

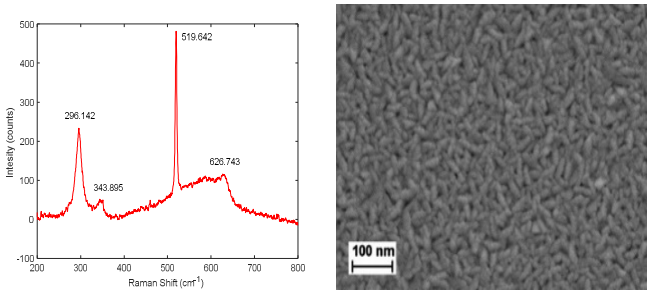

(a) (b)

Fig. 5. CuO characterization: (a) Raman spectra, and (b) SEM image of CuO.

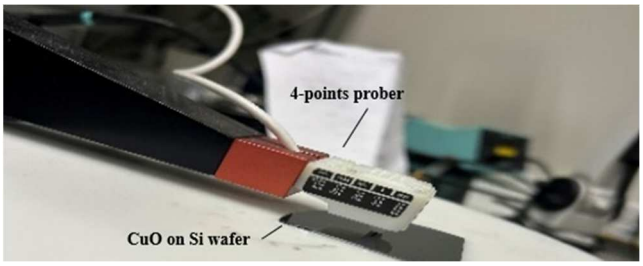

Fig. 6. Four-points prober for CuO electrical characterization.

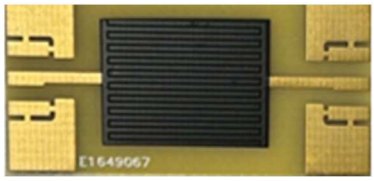

Fig. 7. Top view of the fabricated sensor covered with cupric oxide.

The Agilent E5061B-3L5 enhanced network analyzer (ENA), available at the WELCOME characterization platform at UCLouvain, was utilized to assess the electrical response of both the blank and the CuO-coated structures. The sensor basic impedance was extracted from the scattering parameters S to analyze the capacitance and resistance variations (between the blank structure and the CuO- coated sensor) in the frequency range of 100 kHz to 3 GHz.

Fig. 8a and Fig. 8b, respectively, show the effective capacitance and parallel resistance curves. The effect of the CuO layer is evident in the change in capacitance from 10.35 pF to 11.67 pF due to the change in permittivity. In addition, a significant shift in the parallel resistance R_d is observed, which increased from 2.27 kΩ to 49.30 kΩ. TABLE *II* summarizes the changes in various electrical parameters, i.e., C_{eff}, R_s, R_d, L_s and the resonant frequency f_0 which were calculated from (7) (8) (9) (10) [16], where Y_{12} and Y_{21} are the measured two-port admittances of the sensor.

$$C_{eff} = -\frac{\text{imag}(Y_{12})}{2\pi f} \tag{7}$$

$$Y_{avg} = -\frac{Y_{12}+Y_{21}}{2} \tag{8}$$

$$R_s = \text{Re}\left(\frac{1}{Y_{avg}}\right)_{f\rightarrow \text{high band}} \tag{9}$$

$$R_d = \text{Re}\left(\frac{1}{Y_{avg}}\right)_{f\rightarrow \text{low band}} \tag{10}$$

Gas measurements were subsequently performed on the gas bench available at the WELCOME platform, at room temperature and an initial relative humidity of 50 %. The setup

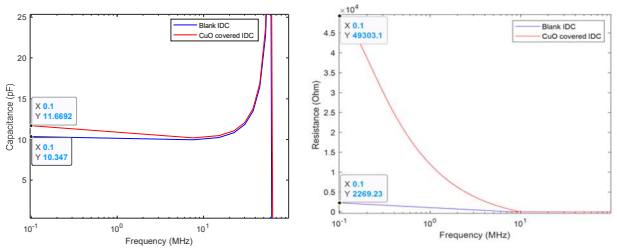

(a) (b)

Fig. 8. The effect of CuO layer on IDC's (a) capacitance, and (b) resistance.

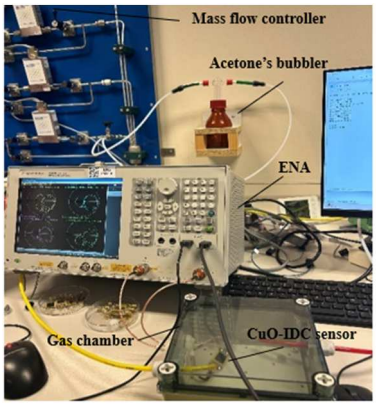

Fig. 9. Gas measurement setup including connection between ENA, gas chamber and MFCs.

TABLE II. THE EFFECT OF CUO ON THE ELECTRICAL PARAMETERS OF IDC.

Structure	Electrical parameters				
	C_{eff} (pF)	R_s (Ω)	R_d (kΩ)	f_0 (MHz)	L_s (nH)
Blank structure IDC	10.35	155.56	2.27	60.1	677.5
IDC_CuO	11.67	116.53	49.3	60.1	600.9

included an ENA network analyzer, a gas chamber, and software to control mass flow controllers (MFCs), timing, and concentrations, as shown in Fig. 9.

Similar to the blank and coated structures, electrical measurements were performed for the sensor when exposed to acetone. The effect of acetone on the sensor capacitance is shown in Fig. 10. There is a noticeable difference between the two pulses of acetone with the increase of the concentration (1 L/min of acetone), in terms of response and recovery time. However, as shown in Fig. 10, the sensor response, calculated using (11), is approximately 0.3 % for the first pulse and 0.63 % for the second one at 7.6 MHz.

$$\text{Sensitivity}\ (\%) = \frac{C_{acetone} - C_{air}}{C_{air}} \times 100 \qquad (11)$$

where $C_{acetone}$ is the sensor capacitance during the gas purge, and C_{air} is the capacitance of the sensing device in air. Other electrical parameters were also measured during acetone exposure. Effective capacitance exhibited the strongest correlation with injected gas concentration, whereas series resistance, parallel resistance, and equivalent inductance showed negligible dependence. The limited capacitance variation arises from the PCB structure's geometric dominance, specifically the sensitive coating's minimal thickness (35× thinner than the metal layer).

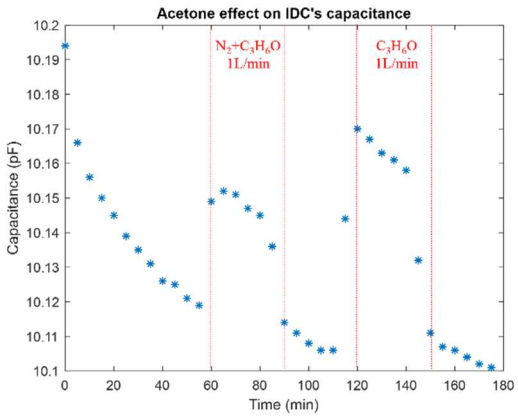

Fig. 10. Acetone's effect on CuO-IDC based sensor.

IV. CONCLUSIONS

We fabricated an acetone gas sensor made of copper oxide (CuO) deposited on an interdigitated structure using the sputtering technique. Characterization of the sensitive layer demonstrated successful fabrication with excellent quality. Electrical measurements using ENA revealed the influence of copper oxide on the IDC capacitance, which shifted slightly from 10.35 pF to 11.67 pF due to a change in the permittivity at the top of the sensor. Gas measurements revealed a variation in capacitance for two consecutive gas pulses with different acetone concentrations of 0.3% for the first pulse and 0.63% for the second pulse. This slight variation in capacitance is attributed to the thinness of the copper oxide layer compared to the thickness of the electrodes (1 µm thick copper oxide layer compared to 35 µm thick printed circuit board). Future work on integrated circuits will take these results into account to improve the performance and design of cupric oxide-based gas sensors and interdigitated capacitors.

ACKNOWLEDGMENT

The authors gratefully acknowledge the support of GreenWin, the Walloon Cleantech innovation cluster, through the MARINA - ModulAR INdoor Air quality management platform towards energy efficient systems and healthy places - project. We also extend our gratitude to Pascal Simon, WELCOME platform manager at UCLouvain.

REFERENCES

[1] H. Mohammadzadeh, H. Mohammadi, M. A. Tavakoli, and S. Sadeghi, "Sudden death due to acetone toxicity," Pharmaceutical and Biomedical Research, 2021.

[2] J. Coonrod, "Benefits of mixed dielectrics when used for high-frequency PCB applications," High Frequency Electronics, vol. 11, pp. 28-36, 2012.

[3] N. Bamiedakis, R. Penty, I. White, T. Hutter, and S. Ellliott, "Low-cost PCB-integrated polymer waveguide sensor for gas detection," in CLEO: Science and Innovations: Optica Publishing Group, p. CThC5, 2011.

[4] N. Bamiedakis, T. Hutter, R. V. Penty, I. H. White, and S. R. Elliott, "PCB-integrated optical waveguide sensors: an ammonia gas sensor," Journal of Lightwave Technology, vol. 31, no. 10, pp. 1628-1635, 2013.

[5] M. Hadj Said, A. Khlifi, N. Zardi, S. Gomri, A. Haj Said, and F. Tounsi, "Toward the use of graphene oxide-based planar inductors as a transducer for gas sensing applications," Smart Science, vol. 12, no. 2, pp. 293-304, 2024.

[6] S. C. Mukhopadhyay, B. George, J. K. Roy, and T. Islam, "Interdigital Sensors," Cham: Springer International Publishing, vol. 36, p. 10, 2021.

[7] Y. R. Choi, Y.-G. Yoon, K. S. Choi, J. H. Kang, Y.-S. Shim, Y. H. Kim, H. J. Chang, J.-H. Lee, Ch. R. Park, S. Y. Kim and H. W. Jang, "Role of oxygen functional groups in graphene oxide for reversible room-temperature NO2 sensing," Carbon, vol. 91, pp. 178-187, 2015.

[8] S. Prezioso, F. Perrozzi, L. Giancaterini, C. Cantalini, E. Treossi, V. Palermo, M. Nardone, S. Santucci and L. Ottaviano, "Graphene oxide as a practical solution to high sensitivity gas sensing," The Journal of Physical Chemistry C, vol. 117, no. 20, pp. 10683-10690, 2013.

[9] A. Kumar, C. Wang, F.-Y. Meng, J.-G. Liang, B.-F. Xie, Z.-L. Zhou, M. Zhaoc and N.-Y Kim, "Aerosol deposited BaTiO3 film based interdigital capacitor and squared spiral capacitor for humidity sensing application," Ceramics International, vol. 47, no. 1, pp. 510-520, 2021.

[10] N. S. Mazlan, M. M. Ramli, M. M. A. B. Abdullah, D. S. C. Halin, S. S. M. Isa, L. F. A. Talip, N. S. Danial and S. A. Z. Murad, "Interdigitated electrodes as impedance and capacitance biosensors: A review ", 3rd electronic and green materials international conference 2017 (EGM 2017), Thailand, 2017.

[11] M. R. Mullen and P. K. Dutta, "Building selectivity for NO sensing in a NOx mixture with sonochemically prepared CuO structures," Chemosensors, vol. 4, no. 1, p. 1, 2015.

[12] F. Akhter, M. E. E. Alahi, H. R. Siddiquei, C. P. Gooneratne, and S. C. Mukhopadhyay, "Graphene oxide (GO) coated impedimetric gas sensor for selective detection of carbon dioxide (CO 2) with temperature and humidity compensation," IEEE Sensors Journal, vol. 21, no. 4, pp. 4241-4249, 2020.

[13] F. Khurshid, M. Jeyavelan, T. Hussain, M. S. L. Hudson, and S. Nagarajan, "Ammonia gas adsorption study on graphene oxide based sensing device under different humidity conditions," Materials Chemistry and Physics, vol. 242, p. 122485, 2020.

[14] A. Rydosz, "The use of copper oxide thin films in gas-sensing applications," Coatings, vol. 8, no. 12, p. 425, 2018.

[15] A. Szkudlarek, K. Kollbek, S. Klejna, and A. Rydosz, "Electronic sensitization of CuO thin films by Cr-doping for enhanced gas sensor response at low detection limit," Materials Research Express, vol. 5, no. 12, p. 126406, 2018.

[16] T. Zheng, M. Han, G. Xu, and L. Luo, "Design and fabrication of suspended high Q MIM capacitors by wafer level packaging technology," in 2015 16th International Conference on Electronic Packaging Technology (ICEPT), pp. 89-94, 2015.

[17] C. Dias and R. Igreja, "A method of recursive images to obtain the potential, the electric field and capacitance in multi-layer interdigitated electrode (IDE) sensors," Sensors and Actuators A: Physical, vol. 256, pp. 95-106, 2017.

[18] L. Q. Jun, G. W. bin Djaswadi, H. F. bin Hawari, and M. A. B. Zakariya, "Simulation of interdigitated electrodes (IDEs) geometry using COMSOL multiphysics," in 2018 International Conference on Intelligent and Advanced System (ICIAS), pp. 1-6, 2018.

[19] X. Zeng, "Fabrication and characterization of opto-electronic devices based on p-type thin-film semiconductors," UCL-Université Catholique de Louvain, 2022.

[20] A. S. Zoolfakar, M. Z. Ahmad, R. A. Rani, J. Z. Ou, S. Balendhran, S. Zhuiykov, K. Latham, W. Wlodarski and K. K.-zadeh, "Nanostructured copper oxides as ethanol vapour sensors," Sensors and Actuators B: Chemical, vol. 185, pp. 620-627, 2013.